Electronic Supplementary Material (ESI) for Physical Chemistry Chemical Physics.

Supporting Information

Perfect Planar Tetra-Coordinated MC_6 Monolayer: Superior Anode Material for Li-ion Battery

Shaohua Lu, Chuncheng Yang, Dong Fan, and Xiaojun Hu*

College of Materials Science and Engineering, Zhejiang University of Technology, Hangzhou 310014, China

AUTHOR INFORMATION

*E-mail: huxj@zjut.edu.cn (X.J. Hu)

Structure Prediction Parameters

The Crystal structure AnaLYsis by Particle Swarm Optimization (CALYPSO) code [1, 2]within the particle swarm optimization (PSO) method was employed to find the global minimum of two-dimensional MC_6 (M = Cu, Ag, Au) systems. Unit cells containing no more than 4 formula units (*f.u.*) were considered. In the first step, random structures with certain symmetry are constructed and crystallographic symmetry operations are employed to generate atomic coordinates. Two-step local optimization using the *ab initio* Vienna Simulation Package (VASP) code[3] were performed with the conjugate gradients method and stopped when the convergence criterion was reached. The value of *DeltaZ (important input parameter in CALYPSO code)* was set to 1.0, which means that the atomic deviation along vacuum layer can reach 1.0 Å. *PREC, EDIFF, NSW,* and *KSPACING* (input parameter in VASP code) were set to *Normal (Accurate), 3E-2 (1E-3), 45 (100), 0.8 (0.5)* for each step, respectively. After generating the first generation structures by PSO, 60 % of the structures with lower total energies were selected to construct the next generation structures by PSO. The rest part of structures (40 %) in the new generation were randomly generated. Bond characterization matrix using a structure fingerprinting technique was applied to the generated structures, which guarantee that identical structures were strictly forbidden. These procedures largely improve the diversity of the structures, which was crucial for structural global search efficiency. In most cases, structure searching simulations for each calculation were stopped after 1000-1200 structure were generated (e.g. about 20-30 generations).

Table S1. The detailed geometry parameters for optimized MC_6 monolayers

Phase	Space Group	Lattice Parameters (Å)		Atomic Positions (Fractional coordinates)		
			Atom	x	y	z
CuC_6	*Pmmm*	a=5.40 b=4.24 c=15 α=β=γ=90º	Cu	0.00000	0.00000	0.50289
			C	0.50000	0.83030	0.50284
				0.50000	0.16970	0.50284
				0.73524	0.33779	0.50286
				0.26476	0.66221	0.50286
				0.26476	0.33779	0.50286
				0.73524	0.66221	0.50286
AgC_6	*Pmmm*	a=5.70 b=4.16 c=15 α=β=γ=90º	Ag	0.00000	0.00000	0.49666
			C	0.50000	0.83065	0.49664
				0.50000	0.16935	0.49664
				0.72092	0.33739	0.49665
				0.27908	0.66261	0.49665
				0.27908	0.33739	0.49665
				0.72092	0.66261	0.49665
AuC_6	*Pmmm*	a=5.64 b=4.15 c=15 α=β=γ=90º	Au	0.00000	0.00000	0.49664
			C	0.50000	0.82986	0.49665
				0.50000	0.17014	0.49665
				0.72409	0.33581	0.49665
				0.27591	0.66419	0.49665
				0.27591	0.33581	0.49665
				0.72409	0.66419	0.49665

Table S2. Detailed parameters for computational tasks.

Computational Tasks	Functional	K-points (2π/Å)	Cutoff Energy (eV)	Energy Convergence Criteria (eV)	Force Convergence Criteria (eV/Å)
Geometry Optimization	GGA+PBE	0.03	650	10^{-6}	10^{-3}
Band Structure	HSE06	20 points between two high symmetry points	550	10^{-4}	-
Density of state	HSE06	0.02	550	10^{-4}	-
Molecular Dynamical	GGA+PBE	0.06	500	10^{-3}	-
Phonon Dispersion Curves	GGA+PBE	0.03	650	10^{-8}	10^{-7}
Geometry Optimization (Li-adsorbed systems)	GGA+PBE	0.04	650	10^{-4}	0.01
CI-NEB	GGA+PBE	0.04	650	10^{-4}	0.02

Table S3. The calculated elastic constants for MC_6 monolayers

	C_{11}/GPa	C_{22}/GPa	C_{12}/GPa	C_{21}/GPa	C_{66}/GPa
CuC_6	615	1169	311	311	479
AgC_6	846	1224	439	439	502
AuC_6	1088	1503	511	511	607

Table S4. The calculated lattice constants before (after) geometry optimization and lattice expansion for MC_6 monolayers

	Lattice constants before geometry optimization		Lattice constants after geometry optimization		Lattice expansion	
	a/Å	b/Å	a/Å	b/Å	a	b
CuC_6	10.80	8.49	11.48	8.51	6.30 %	0.24 %
AgC_6	11.40	8.32	11.59	8.63	1.67 %	3.73 %
AuC_6	11.28	8.30	11.27	8.55	0.08 %	3.01 %

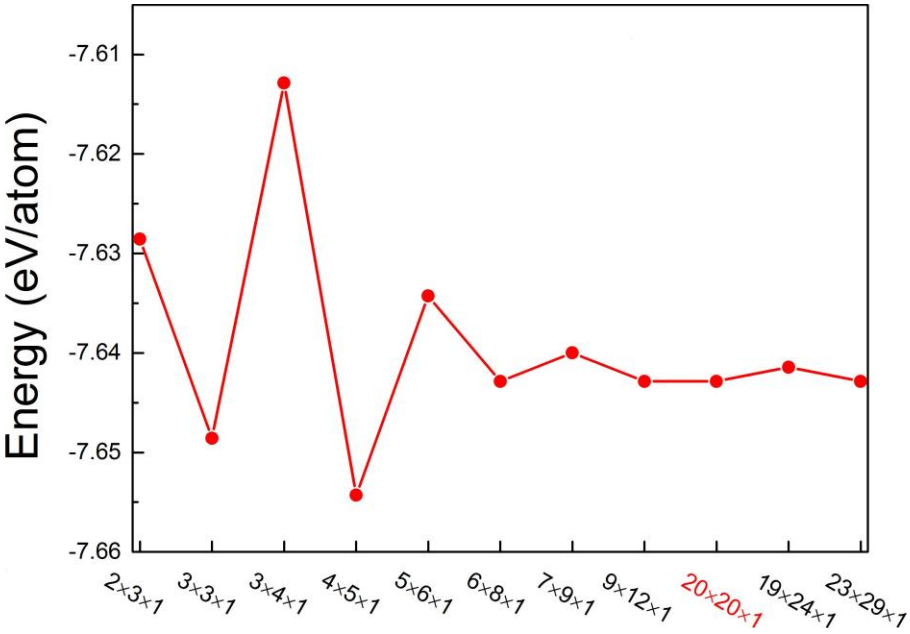

Figure S1. The calculated total energies per atom as a function of k-points.

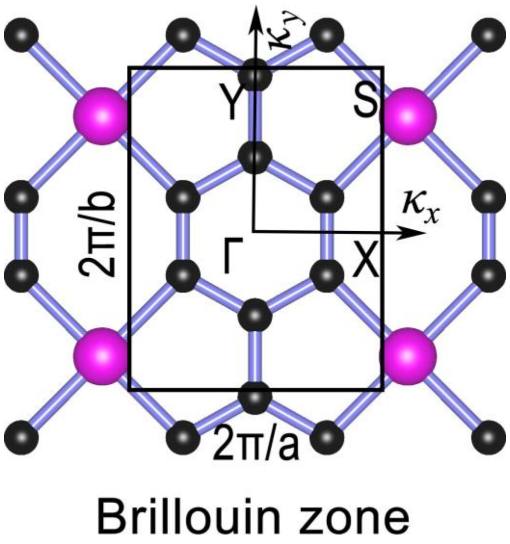

Figure S2. The Brillouin zone for MC_6 monolayer. The four high symmetry points are Γ(0, 0, 0), Y(0, 1/2, 0), S(1/2, 1/2, 0), X(1/2, 0, 0).

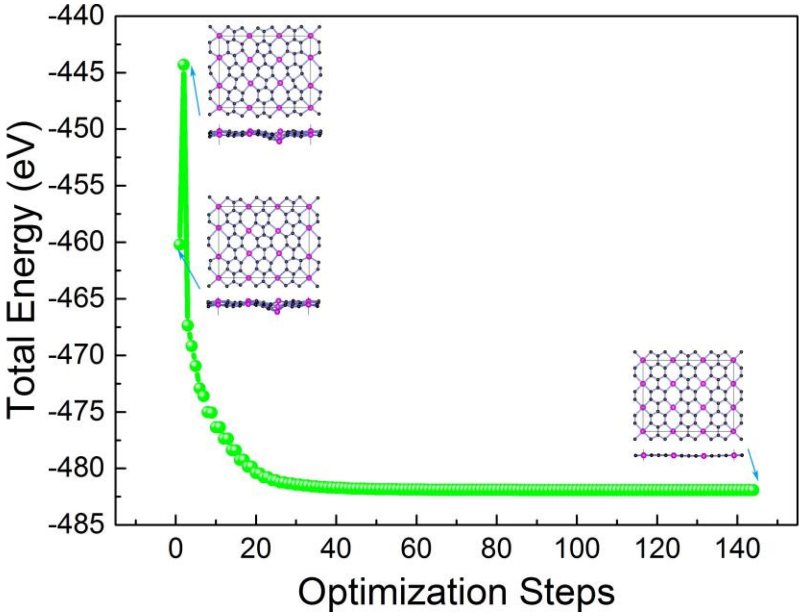

Figure S3. The fluctuations of the total energy for the final configuration (3×3 supercell)) from high temperature (1500 K) AIMD simulation as a function of the optimization steps with some random atoms out of the basal plane. The insets represent the top and side views of the structure at the optimization step pointed by blue arrowed lines. No symmetry restriction was considered during the geometry optimization.

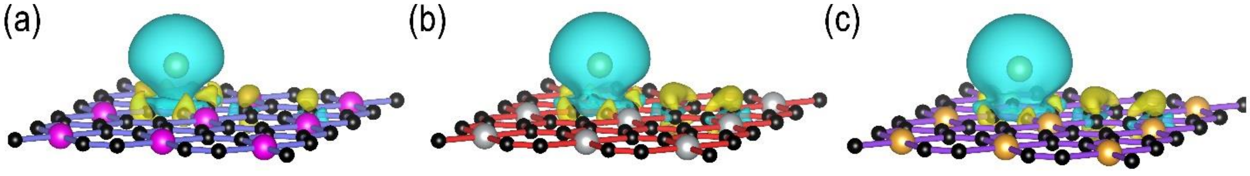

Figure S4. The charge density difference plots of the Li-adsorbed MC_6 monolayers. (a) CuC_6, (b) AgC_6, (c) AuC_6. The charge density difference plots were calculated by the following equation: $\rho = \rho_{Total} - \rho_{MC_6} - \rho_{Li}$. Where ρ_{Total}, ρ_{MC_6}, and ρ_{Li} are the total charge of the Li-adsorbed system, MC_6, and single Li atom. The yellow (blue) colored cloud represents the gains and loses of the electron.

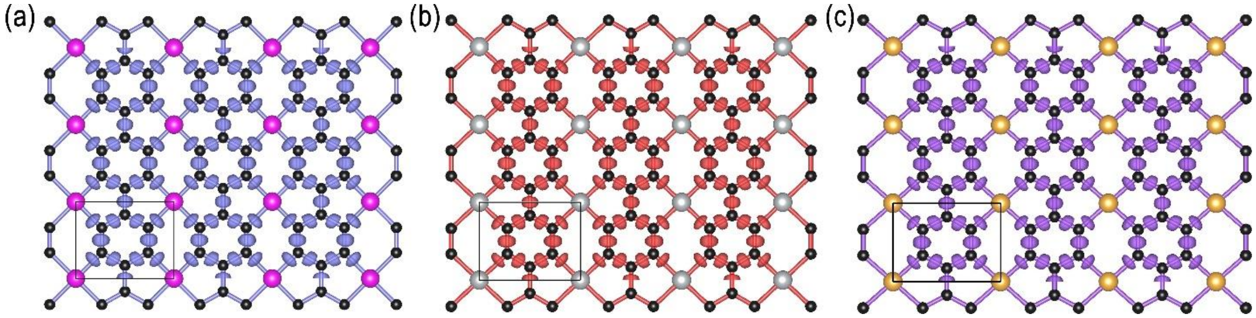

Figure S5. Plot of the calculated electron localization function (top view) for (a) CuC_6, (b) AgC_6, (c) AuC_6, colored cloud represent the localization of electron.

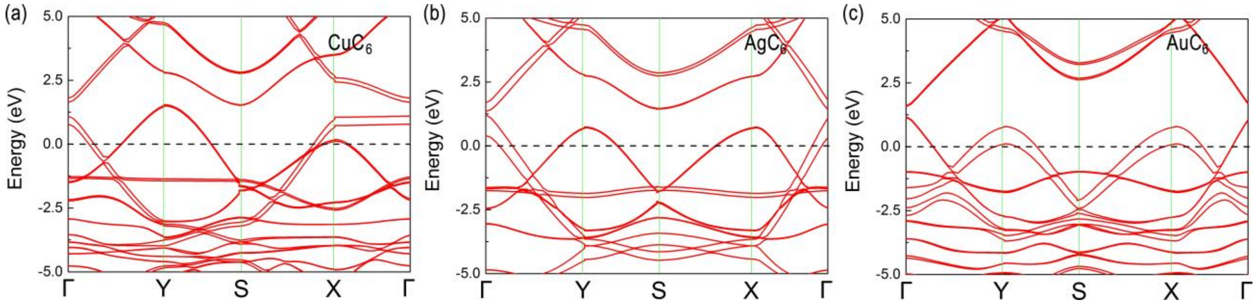

Figure S6. The calculated band structure for MC_6 monolayers considering spin-orbit coupling. The Fermi level was set to 0 eV.

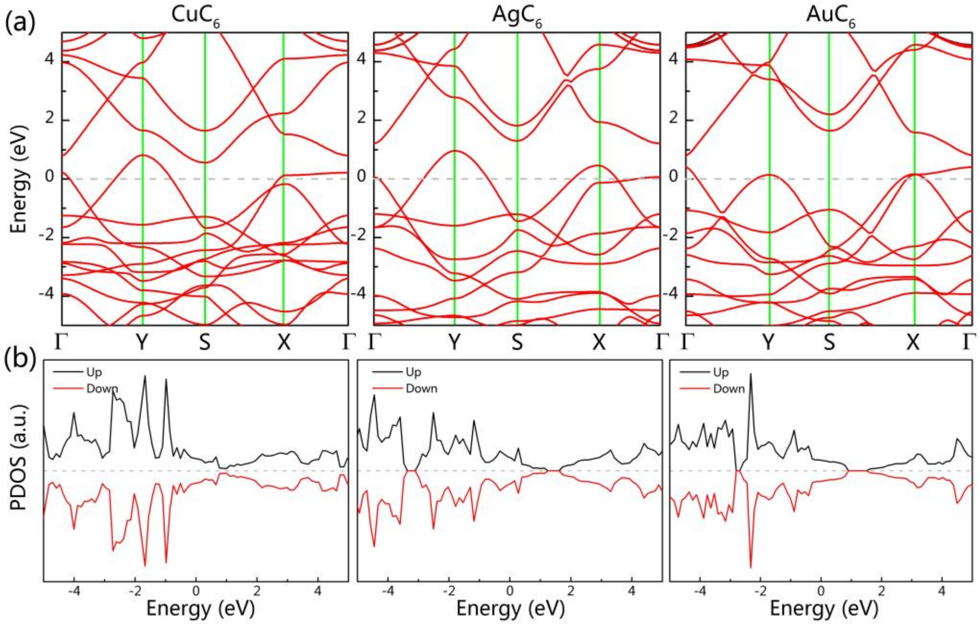

Figure S7. (a) Spin-unrestricted band structure for MC_6 monolayers. (b) Calculated density of state for spin-up and spin-down states of MC_6 monolayers.

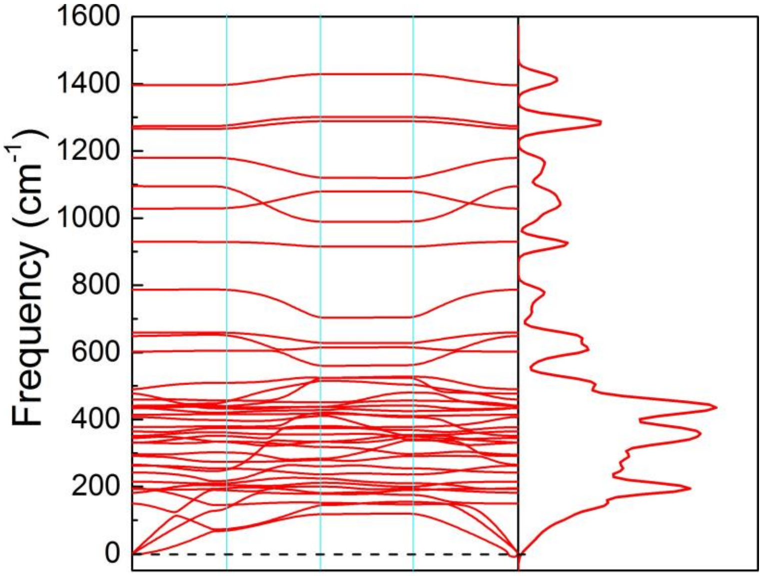

Figure S8. Phonon dispersion curves and phonon density of state for CuC_6Li_6 (highest concentration of Li-ion adsorption on CuC_6 electrode).

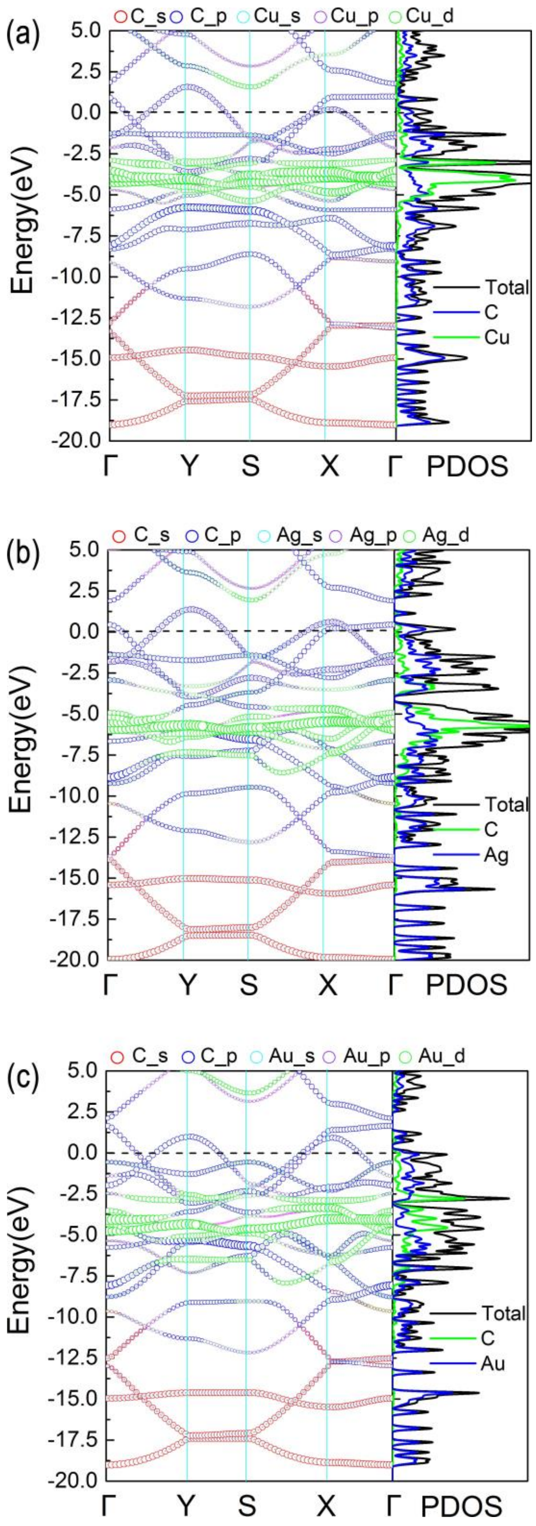

Figure S9. Orbital-resolved band structure and partial density of state divide into C and M atoms of the (a) CuC_6, (b) AgC_6, and (c) AuC_6 at a wider energy range from -20 to 5 eV. Colored hollow sphere represent the contribution of different atomic orbitals. The Fermi level was set to 0 eV.

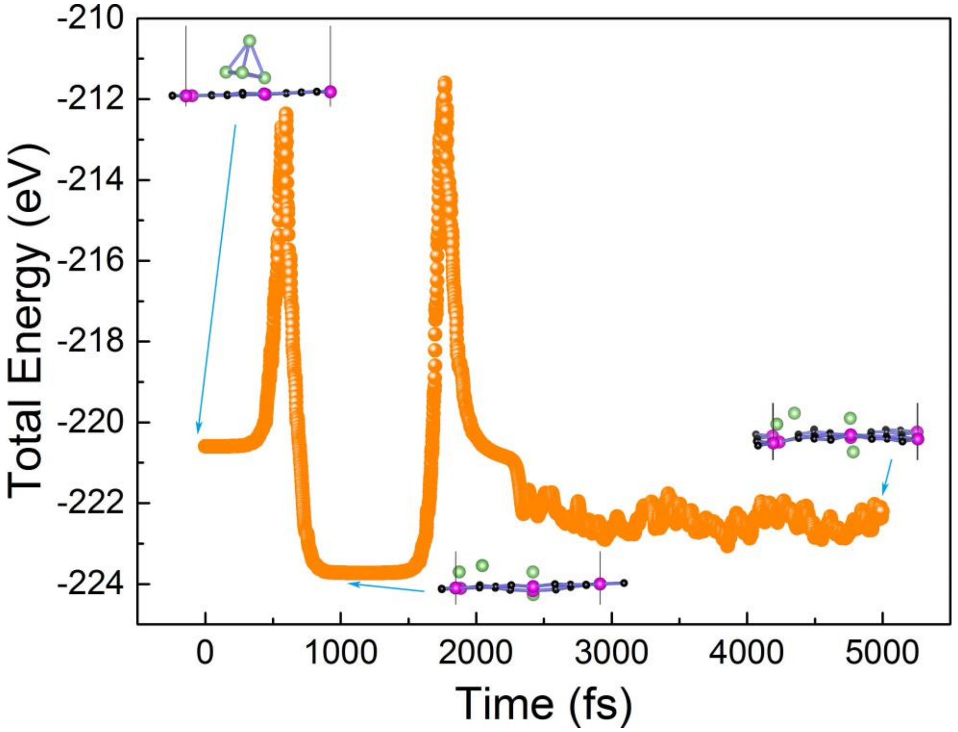

Figure S10. The fluctuations of the total energy of Li_4 cluster adsorbed CuC_6 supercell as a function of the molecular dynamics simulation times under 300 K. The insets represent the top and side views of the structures at the simulation time pointed by blue arrowed lines.

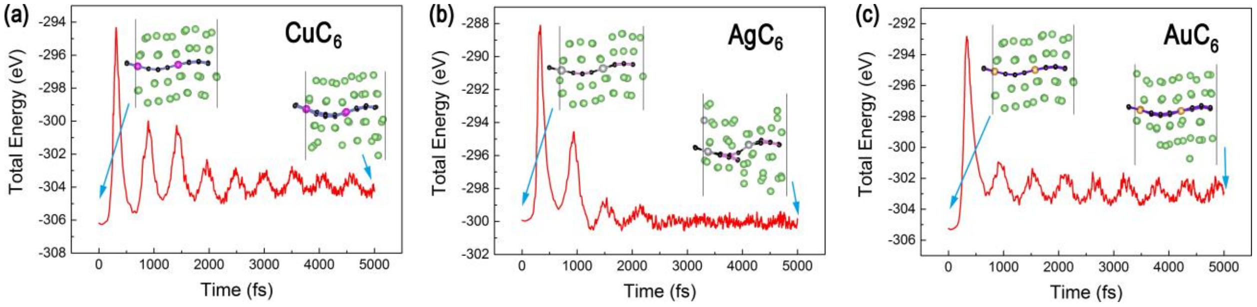

Figure S11. The energy profile versus simulation time for systems with two layers of Li-ions on both sides of (a) CuC_6, (b) AgC_6, and (c) AuC_6 systems under 300 K. The insets was the starting and final geometries for Li-ion adsorbed systems.

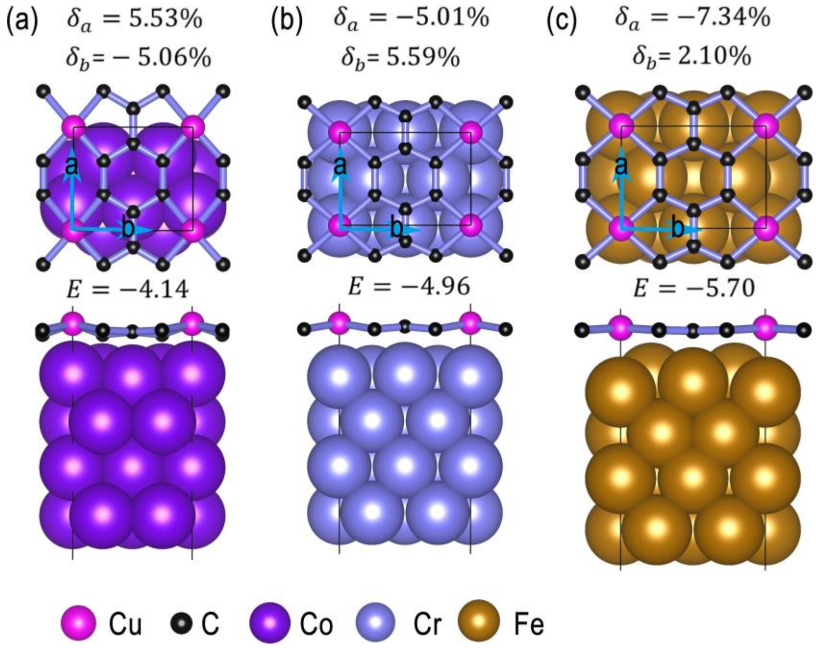

Figure S12. Top and side views of the respective CuC_6 on (a) Co (100), (b) Cr (100), (c) Fe (100). The comparisons of the lattice mismatches and adsorption energies of the CuC_6 on the corresponding substrate was shown in the upper panel. Here, $\boldsymbol{a}$ ($\boldsymbol{b}$) is the lattice constant of the corresponding substrate, the different δ (%) values measure the different lattice dismatches for the systems, and E_{ad} (DFT-D2 correction was applied measures the corresponding adsorption energies per unit cell).

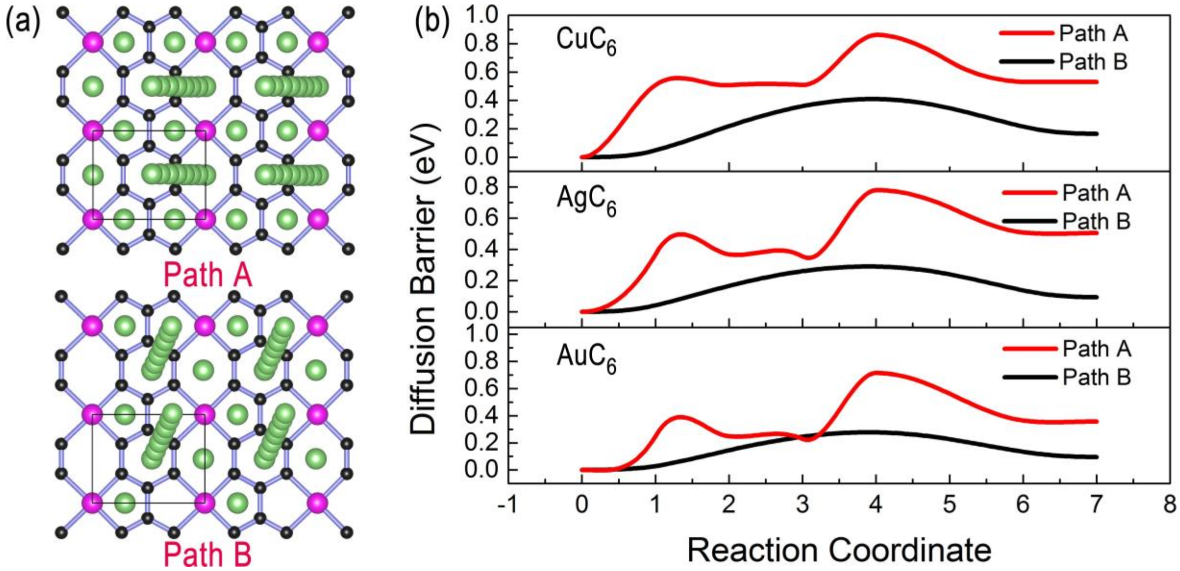

Figure S13. (a) The scheme for the diffusion paths, marked as Path A and Path B. (b) Calculated diffusion barrier in different MC_6 systems for Path A and Path B, respectively.

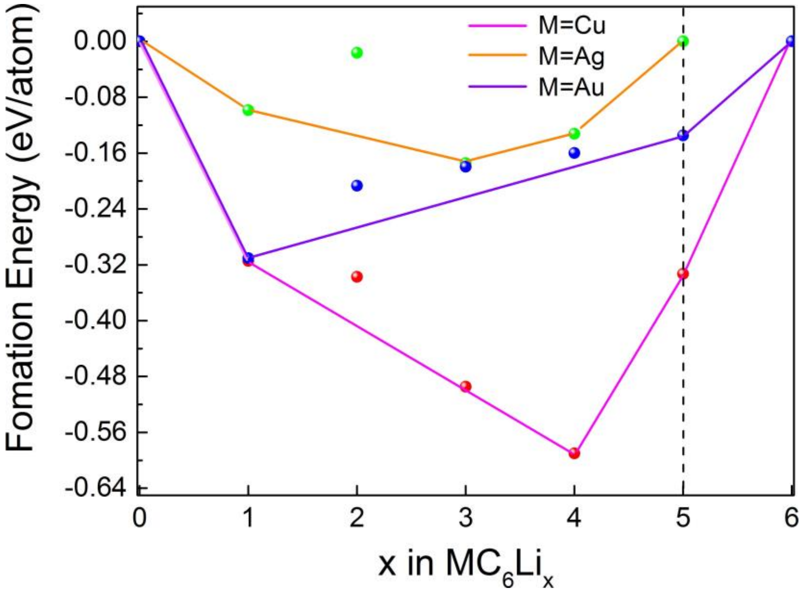

Figure S14. The fluctuations of formation energy as a function of x in MC_6Li_x. The colored balls represent the value of formation energy when x equals 1, 2 ... 6. The colored lines form the convex hull for stable phases in the whole composition range of MC_6Li_x.

Reference

[1] Wang Y, Lv J, Zhu L, Lu S, Yin K, Li Q, et al. Materials discovery via CALYPSO methodology. Journal of physics Condensed matter : an Institute of Physics journal 2015;27:203203.

[2] Wang YL, J. Zhu, L. Ma, YM. CALYPSO a method for crystal structure prediction. COMPUTER PHYSICS COMMUNICATIONS 2012;183:2063-70.

[3] Kresse GF, J. Efficient iterative schemes for ab initio total-energy calculations using a plane-wave basis set. PHYSICAL REVIEW B 1996;54:11169-86.